

Thermophysical Properties and Phase Changes in the Upper Mantle

Sayyadul Arafin¹

Received: 6 January 2015 / Accepted: 5 August 2015 / Published online: 14 August 2015
© Springer Science+Business Media New York 2015

Abstract The correlation between phase changes within the upper mantle and the thermophysical properties of the minerals therein has been investigated by using the thermoelastic and thermodynamic equations. The depth dependence data of seismic velocities of Jeffreys–Bullen and density within the upper mantle are used as inputs in the analysis. The material characteristic properties like Debye temperature, Θ_D , adiabatic compressibility, κ_S , Grüneisen parameter, ξ , and the specific heat capacity, C_P computed as a function of depth show clearly two discontinuities at average depths of 414 km and 645 km which are in fair agreement with the presently accepted depths 410 km and 670 km from the preliminary reference earth model data.

Keywords Density · Olivine · Phase changes · Seismic velocities · Thermophysical properties · Upper mantle

1 Introduction

Our knowledge about the deep interior of the earth is derived mostly from seismological data. However, geochemical and mineral physics data are becoming increasingly important lately in the understanding of the interior of the earth. Seismological observations of the early twentieth century provide us with the concept of a layered earth composed of a thin crust, a mantle, a liquid outer core, and a solid inner core. The interpolated observed travel-time tables of Jeffreys and Bullen [1] played a vital role during the first half of the twentieth century in developing the one-dimensional (1D)

✉ Sayyadul Arafin
sayfin@squ.edu.om

¹ Physics Department, College of Science, Sultan Qaboos University, Box: 36, Al-Khoudh, 123 Muscat, Oman

seismic velocity models including the classic Jeffreys–Bullen–Gutenberg model for the entire earth [2]. The Jeffreys–Bullen model of the earth predicts that the transition zone is spread over an interval between 413 km and 983 km of the interior of the earth. According to this model, the velocity and density gradients, although high, decrease with depth in this interval of depth. While working with Adams–Williamson equation to account for the moment of inertia of the earth, it was found that an unacceptable concentration of mass needed to be considered in the outer core relative to the inner core [3]. This difficulty was avoided by assigning additional mass to the region of the mantle between 400 km and 900 km below the surface of the earth which was considered as a region of inhomogeneity. This inhomogeneity was due to a progressive change of mantle material to high-pressure phases [3]. Evidence from surface wave dispersion and free oscillation periods led to the conclusion that density changes due to phase transitions in the upper mantle are concentrated in relatively narrow depth ranges at 350 km to 400 km and 700 km [4, 5]. According to Stacey [3], the earth model produced from *P* and *S* wave velocities [4–6] will change only in minor ways in the future.

Preliminary reference earth model (PREM) in [7] is a one-dimensional earth model representing the average earth properties as a function of the earth's radius. This model was designed to fit a variety of different datasets, including free oscillation center frequency measurements, surface wave dispersion observations, travel-time data for a number of body-wave phases, and basic astronomical data such as the Earth's radius, mass, and moment of inertia. The assumption of anelastic dispersion and anisotropy in the 3D heterogeneous earth makes the model frequency-dependent and transversely isotropic for the upper mantle. The introduction of transverse isotropy in the upper mantle was necessary to account for the shorter period fundamental toroidal and spheroidal modes. It is widely used in seismology and geodynamics for computing free oscillations and long-period seismic motions and as the 1D reference structure in 3D tomographic inversions.

Significant progress in our understanding of the fundamental global scale dynamic processes of the Earth's interior can only be achieved through an integrated, multidisciplinary approach, combining knowledge and latest achievements in geochemistry, geodynamics, geomagnetism, seismology, and mineral physics [2]. Presently, considerable work has been progressing towards developing reference 3D models of the earth by following this multidisciplinary approach.

Thermoelastic and thermodynamic properties of rocks and minerals provide information to study the deep interior of the Earth and are of considerable significance for deriving the mineralogical and compositional models of Earth's mantle. At depth level less than 700 km, the thermophysical properties can help determine the tectonic and petrogenic processes involved in the generation of oceanic lithosphere. In addition to that thermoelastic properties can enhance our knowledge about the formation and transformation of rocks and minerals. Knowledge of the physical properties of mantle minerals provides the essential link between geophysical observations and geodynamics [8]. The tools and concepts of thermodynamics are an essential part of any model of planetary evolution, dynamics, and structure.

With the advancement of technology it is now possible to measure elastic properties at high pressures using X-ray diffraction, inelastic X-ray scattering, ultrasonic

interferometry, and Brillouin spectroscopy. Due to the complexity of these techniques, these have not been widely used in characterizing upper mantle rocks [9]. Most of the Earth is solid, and much of it is at temperatures and pressures that are difficult to achieve in the laboratory. Nevertheless, the usual practice is to formulate a reasonable model to extrapolate the laboratory measurements.

Mineral physics, partial melting, and solid–solid phase changes play a vital role in understanding the composition of the mantle. The variations in densities and seismic velocities of rocks with temperature, pressure, and composition are usually very small. However, an extreme change in mineralogy can change density and seismic velocity appreciably. Like velocity and density, the proportions and compositions of the various phases or minerals that determine the physical properties of rocks depend on temperature, pressure, and composition as well.

In the present work, we have used the seismic velocities such as p - and s -wave velocities given in [1] and the density data of [10] to obtain the useful thermoelastic and thermodynamic properties like Debye temperature, adiabatic compressibility, Grüneisen parameter, and specific heat capacity of the Earth's mantle by utilizing thermoelastic and thermodynamic equations. Both sets of input data are fairly smooth. The purpose of the present study is to investigate if the thermophysical properties determined from these data are capable of identifying the mantle discontinuities. Section 2 describes, in brief, phase changes in the upper mantle, mathematical formalism is presented in Sect. 3, and results and discussions are given in Sect. 4 followed by summary and conclusions in Sect. 5.

2 Phase Changes in the Upper Mantle

Mantle of the Earth is composed of silicate minerals rich in magnesium. It is subdivided into upper and lower mantle, based upon the changes in seismic wave velocity. Unlike the lower mantle, the upper mantle is non-convecting. The upper mantle comprises the lower part of the lithosphere. The low velocity layer (50 km to 220 km depth) beneath the lithosphere is termed as asthenosphere. The transition zone is characterized by 410 km discontinuity, formed as result of olivine to wadsleyite transition (α to β), and 660 km discontinuity, believed to be caused by the ringwoodite dissociation into ferropericlase and perovskite (γ -dissociation). These discontinuities are called seismic density and velocity discontinuities.

Olivines, the most important rock-forming mineral group within the upper mantle, constitute about 80% of the upper mantle rocks. The composition of most olivines can be represented in the system $\text{Ca}_2\text{SiO}_4\text{--Mg}_2\text{SiO}_4\text{--Fe}_2\text{SiO}_4$. The undifferentiated upper mantle has the basic chemical composition of three parts of dunite to one part of basalt. Pyrolites belonging to this model composition have the ability to crystallize in one of four distinct mineral assemblages [11]: (i) olivine + amphibole, (ii) olivine + plagioclase + pyroxenes, (iii) olivine + aluminous pyroxenes + spinel, or (iv) olivine + pyrope garnet + pyroxenes. This ability of pyrolite facilitates large-scale mineralogical zoning in the upper mantle that will have an important effect on seismic velocities and density.

Much of the variation in the mantle physical properties is in the form of mineralogical phase changes related to increasing pressure with depth. Below the low velocity zone (50 km to 220 km depth), upper mantle mineralogy is dominated by two sets of phase transformations: (i) the olivine-spinel transitions and (ii) the eclogite–garnetite transitions. In the former, the phase of olivine transforms to the γ spinel structure (ringwoodite) with increasing depth, passing through the intermediate β modified-spinel structure (wadsleyite) in compositions with high Mg/Fe ratios. Compression of olivine's atomic structure to its spinel phases under extreme pressure causes a seismic discontinuity at approximately 390 km to 450 km with a net 6% increase in density. This discontinuity corresponds to a transition from the α - to β -structures of multi-component olivine. An experimental phase equilibrium study of the olivine-spinel transitions [12] confirms that the α -olivine to β -modified-spinel transition occurs exothermically (i.e., with positive $P-T$ slope) at pressures and temperatures appropriate to approximately 400 km depth. The $\text{Mg}_2\text{SiO}_4\text{--Fe}_2\text{SiO}_4$ system provides the first-order understanding of seismic discontinuities near 410 km and 660 km depth [8].

Below the depth range of 390 km to 450 km, the main minerals are garnet and spinel. The material has a similar overall composition but the minerals have a more compact structure. At the depth around 670 km, the transformation is fundamentally different from the α - to β -transition, because it involves a change in chemical composition. The olivine and pyroxene–garnet components transform into magnesio-wüstite, $(\text{Mg,Fe})\text{O}$, and perovskite with $\sim 10\%$ density increase across the 1 km to 2 km thick phase change region.

3 Formalism

We discuss the important thermoelastic and thermodynamic equations such as Debye temperature, adiabatic compressibility, Grüneisen parameter, and specific heat capacity, which are used here to investigate their contributions to the understanding of the phase changes within the upper mantle of the Earth.

3.1 Debye Temperature

The Debye temperature, Θ_D , is the temperature corresponding to the highest normal mode of vibration, which is given by

$$\Theta_D = \frac{h\nu_m}{k}, \quad (1)$$

where h is Planck's constant, k is Boltzmann's constant, and ν_m is the Debye frequency.

The Debye temperature, Θ_D , occurs as one of the important ingredients in geophysical studies to investigate the material properties of rocks and minerals. It facilitated the characterization of rocks, minerals, and even geological processes such as metamorphism. It provides important information [13] on the structural stability, bonding strength between the separate elements, structure defects availability including dislocations in crystalline structure of mineral grains, pores, microcracks, and density. Any

change in the external conditions of rocks and other material formation and transformation can lead to a change in the Debye characteristic temperature. Interpretation of Debye characteristic temperature can help estimate [13] the formation and transformation conditions of rocks and ores. The difference between the Debye temperatures of the separated facies of the metamorphic rocks is maximum in case of regional metamorphism, lower at intermediate level of metamorphism, and minimum in case of extremely altered rocks.

Θ_D is calculated from the measured data of density and the seismic velocities such as primary wave (p -wave) and secondary wave (s -wave) velocities in the solid. Without going into the detailed formulation, the working formula for Debye temperature for isotropic solids is given as [14]

$$\Theta_D = 251.2 \left[\frac{\rho}{\mu} \right]^{\frac{1}{3}} v_m, \quad (2)$$

where μ is the mean atomic weight given by M/p , M is the molecular weight, and p is the atomic number. The value of μ for minerals important to the earth's mantle does not vary much from 21 amu [15], ρ is the density in $\text{g}\cdot\text{cm}^3$. v_m is the generalized mean velocity in $\text{km}\cdot\text{s}^{-1}$ of the seismic p - and s -waves. It is given by

$$v_m = \left\{ \frac{1}{3} \left(v_p^{-3} + 2v_s^{-3} \right) \right\}^{-\frac{1}{3}} \quad (3)$$

Here, v_p and v_s are the primary and secondary seismic velocities, respectively.

3.2 Adiabatic Compressibility

The adiabatic or isentropic compressibility, κ_S , can be calculated [14] by using the measured values of v_p and v_s ,

$$\kappa = \frac{1}{\rho \left(v_p^2 - \frac{4}{3} v_s^2 \right)} \quad (4)$$

For rocks, minerals, and other solids, values of adiabatic and isothermal compressibilities differ by about 1 % [15].

3.3 Grüneisen Parameter

Grüneisen parameter is a property of materials, which establishes a link between thermal behavior and the elastic response to thermally induced stress of the material. It measures the anharmonic interactions and is of considerable interest for theoretical and experimental studies in solid-state physics. The thermodynamic approach to determine Grüneisen ratio follows the mathematical expressions for entropy of a pure

substance, Maxwell's equations, coefficient of volume expansion, and the isothermal compressibility. The working formula for Grüneisen parameter, ξ , is given in [14]

$$\xi = \frac{\beta}{\rho C_V \kappa_T} = \frac{\beta}{\rho C_P \kappa_S}, \quad (5)$$

where β (K) is the coefficient of volume expansion, ρ is the density, κ_T and κ_S are the isothermal and adiabatic compressibilities, respectively, and C_V and C_P are the specific heat at constant volume and constant pressure, respectively. All the functions on the right-hand side of Eq. 5 can be determined from experiments and hence ξ is directly determinable. Grüneisen parameter generally lies between 1 and 2 for materials of geophysical interest.

3.4 Specific Heat Capacity

Specific heat at constant pressure (C_P) and constant volume (C_V) is intimately related through a standard thermodynamic relation,

$$C_P = C_V + \frac{TV\beta^2}{\kappa_T}, \quad (6)$$

where V is the molar volume, β is the coefficient of volume expansion, and κ_T stands for isothermal compressibility. Further, specific heat and compressibility are related through specific heat ratio, γ , as

$$\frac{C_P}{C_V} = \gamma = \frac{\kappa_T}{\kappa_S} \quad (7)$$

γ plays a vital role in thermophysical characterization. It appears in many fluid equations including the equation of state during a simple compression and expansion process, the equation for speed of sound, and all the equations for isentropic flows and shock waves. On substituting Eq. 7 in Eq. 6 and rearranging the terms, we get

$$C_P = \frac{TV\beta^2}{\kappa_S(\gamma - 1)}. \quad (8)$$

For rocks and minerals, κ_S is larger than κ_T by about 1% [15]. Adiabatic compressibility can be determined from Eq. 4 and hence γ can be estimated. The values of β as a function of temperature are taken from [15]. An average value of β for the upper mantle material may be taken as $2.66 \times 10^{-5} K^{-1}$.

4 Results and Discussions

The seismic velocities, v_p and v_s , chosen in this investigation are the Jeffreys–Bullen data [16], which are smooth relative to the PREM data. The discontinuities shown in

PREM data are very much obvious. One of our objectives is to see if the thermophysical properties like Debye temperature, adiabatic compressibility, Gruneisen parameter, and the specific heat capacity determined from the smooth seismic data of Jeffreys and Bullen are capable of identifying the two discontinuities at the established depths 400 km and 670 km. The density data used here are the average mantle adiabatic data [10].

4.1 Debye Temperature

The Debye temperatures determined from Eq. 2 are plotted in Figs. 1 and 2 as a function of depth and temperature of the upper mantle, respectively. Both the figures show that Debye temperature increases with increasing depth and temperature. This is quite expected since the seismic velocities and density of the upper mantle increase with increasing depth.

The results of Fig. 1 are less noisy in comparison to that of Fig. 2. The two inflection points shown here with arrows correspond to depths 418 km and 660 km. These depths are in good agreement with the established upper mantle discontinuities at 410 km and 670 km

Temperature profile of the depth of the upper mantle was obtained from reference [16]. This was further used to plot Θ_D against temperature in Fig. 2, which shows that Θ_D increases with increasing temperature. It apparently contradicts the results obtained for harzburgite [14], which shows decrease of Θ_D with increasing temperature. The earlier results of harzburgite correspond to material in a single phase. Unlike that phase changes occur in the minerals of upper mantle which are visible from the seismic velocities and hence yield positive slope of Θ_D .

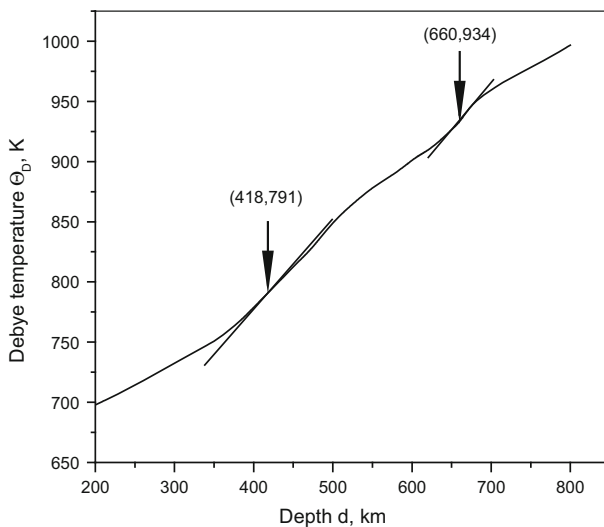


Fig. 1 Variation of Debye temperature with upper mantle depth

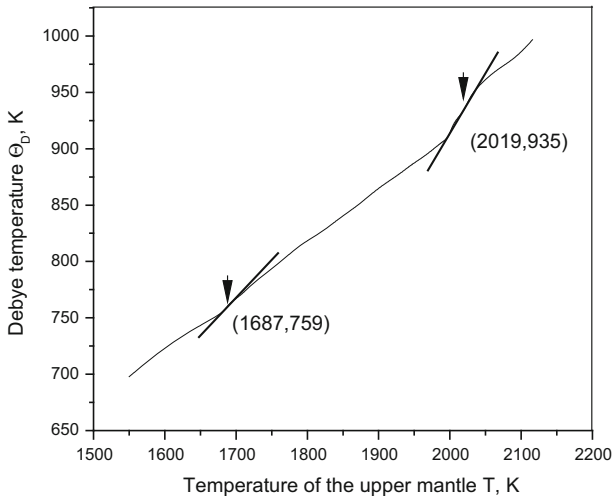


Fig. 2 Variation of Debye temperature with mantle temperature

The inflection points shown in Fig. 2 are less conspicuous than those shown in Fig. 1. Moreover data for the portion of the curve between temperatures 2000 K and 2100 K are noisy so that an average maximum slope is drawn. The two inflection points of Θ_D are found at 1687 K and 2019 K. These temperatures correspond, respectively, to depths 367 km and 660 km.

4.2 Adiabatic Compressibility

The computed values of adiabatic compressibility, κ_S (Fig. 3), decrease with increasing depth. The two discontinuities determined from this plot by locating the inflection points occur at depths 389 km and 658 km with the corresponding κ_S values $5.44 \times 10^{-12} \text{ Pa}^{-1}$ (bulk modulus 184 GPa) and $3.41 \times 10^{-12} \text{ Pa}^{-1}$ (bulk modulus 293 GPa).

4.3 Grüneisen Parameter and Specific Heat Capacity

Grüneisen parameter, ξ , and specific heat capacity at constant pressure, C_P , are determined from Eqs. 5 and 8, respectively. The coefficient of volume expansion, β , occurs as one of the important ingredients to compute ξ and C_P . The measured values [15] of β as a function of temperature were fitted to equation :

$$\beta = 1.52715 + 0.00499 T - 4.005 \times 10^{-6} T^2 + 1.21212 \times 10^{-9} T^3 \quad (9)$$

The original data and the fitted data are plotted in Fig. 4 for the sake of comparison. The values of β at higher upper mantle temperatures are extrapolated from Eq. 9. The computed values of ξ are plotted in Fig. 5, and the values of C_P are plotted in Fig. 6. The inflection points on the curves of ξ and C_P are not as obvious as those for Debye

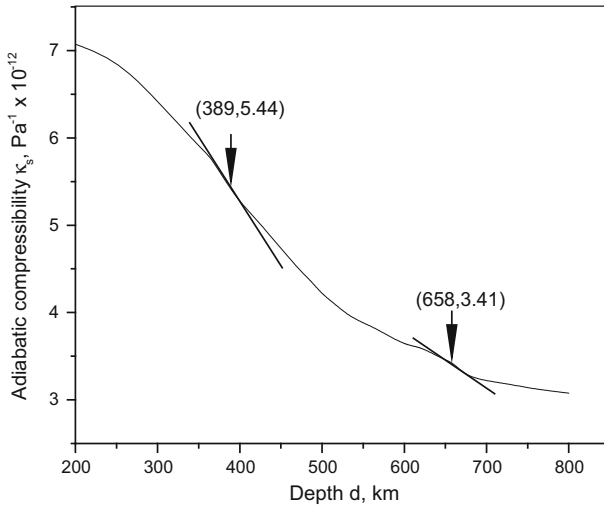


Fig. 3 Variation of adiabatic compressibility within the upper mantle. The discontinuities are shown with the *arrows* at the inflection points

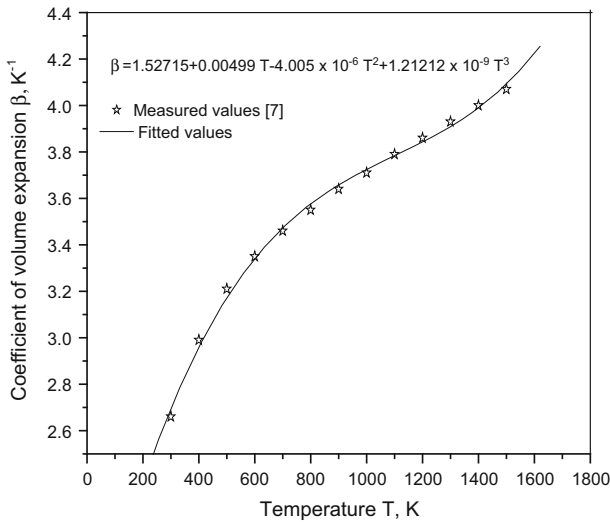


Fig. 4 Coefficient of volume expansion of olivine as a function of temperature

temperatures (Figs. 1, 2) and adiabatic curve (Fig. 3). The ξ curve shows two easily identifiable features—a hump at 400 km and a maximum at 615 km. The diagnostic feature at 400 km is associated with a discontinuity, which is very close to the accepted discontinuity at 410 km. The depths obtained from inflection points are 454 km and 667 km.

The data for C_P curve are especially noisier in the transition zone, i.e., roughly between 400 km and 600 km. Beyond 600 km, both the curves show a lack of clear cut

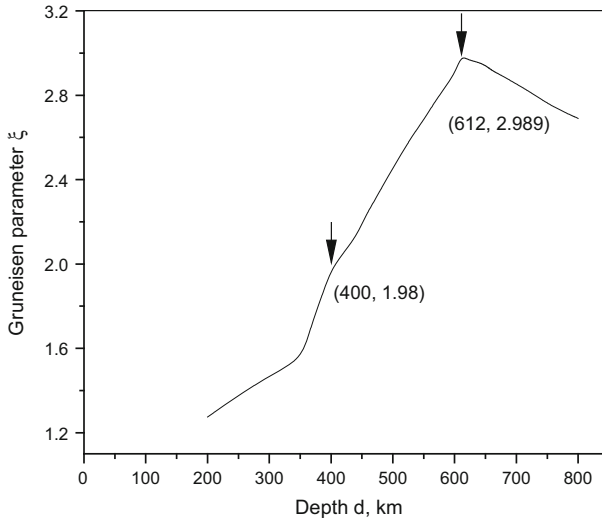


Fig. 5 Grüneisen parameter as a function of depth shows two humps at depths 400 km and 612 km

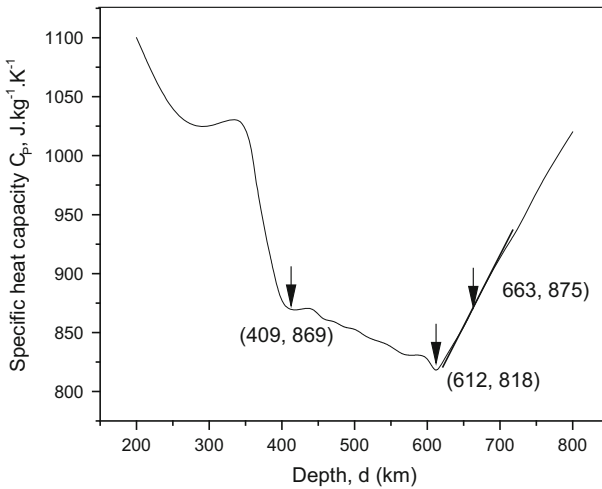


Fig. 6 Specific heat capacity as a function of depth shows two minima at depths 409 km and 612 km. The inflection point indicates a depth of 663 km

inflection points. The C_p values suddenly drop at depths 400 km and 612 km which correspond to humps of the Grüneisen parameter as two maxima at 400 km and 615 km, respectively. Sudden change in specific heat values has also been observed [17] in liquid crystal for phase changes. Similarly large variation in specific heat was depicted for undercooled liquid metals [18, 19]. The gradient of C_p in the undercooled region and the temperature at which C_p undergoes inflection have been related to glass transition temperature [20] of the metals. The inflection point in C_p as well as the characteristic behavior of C_p in the phase change region has been attributed to structural transfor-

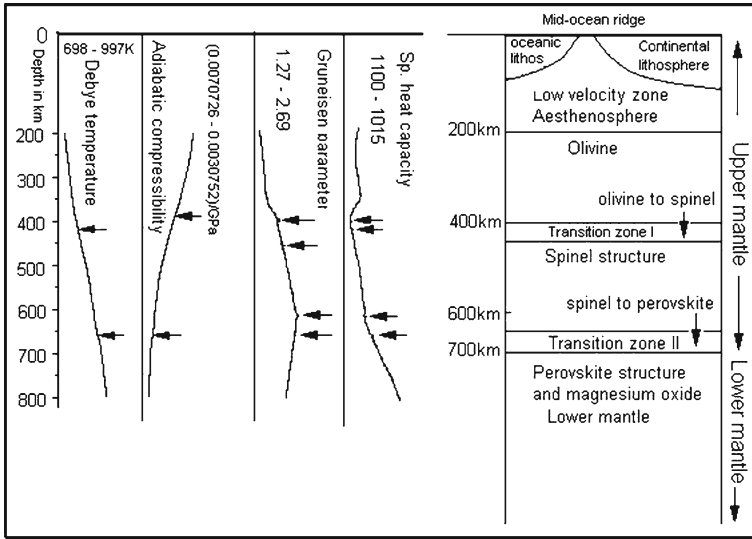


Fig. 7 Correlation of the phase changes of the upper mantle minerals with thermophysical properties

mation of the system. It might be a signature of the configurational transformation. We have observed in the present case that the discontinuities in C_P determined from the inflection points occur at depths 424 km and 658 km. These diagnostic features of maximum and minimum are more easily identifiable in comparison with the inflection points.

5 Summary and Conclusions

We present here a comprehensive diagram (Fig. 7) showing all the plotting of the thermoelastic and thermodynamic properties alongside the different discontinuities of the upper mantle. The minimum and maximum values of each thermophysical quantity are given. The units of the quantities are given in Figs. 1, 3, 5, and 6. Our analysis is focused on mantle materials below depth 200 km. Of all the physical quantities, specific heat capacity and Grüneisen parameter are more deterministic in the sense that they show prominent minima and maxima which are easily identifiable than the inflection points.

The inflection points are easily identifiable from the curves of Debye temperature and adiabatic compressibility unlike the curves of Grüneisen parameter and specific heat capacity, which show the maximum and minimum very clearly. The C_P values suddenly drop at depths 400 km and 612 km which correspond to humps of the Grüneisen parameter as two maxima at 400 km and 615 km, respectively. The average depths determined from the depth dependence of these thermophysical properties are 414 km and 645 km which are in good agreement with the accepted depths of 410 km and 670 km for the corresponding discontinuities in the upper mantle. The study has shown that it is possible to determine the two upper mantle discontinuities from the thermophysical properties by utilizing the smooth geophysical data.

Acknowledgment The author would like to thank Professor Ram N. Singh of the Department of Physics, Sultan Qaboos University for valuable discussions.

References

1. H. Jeffreys, K.E. Bullen, *Seismological Tables* (Black Bear Press, Cambridge, 1940)
2. T. Lay, in *International Handbook of Earthquake and Engineering Seismology*, ed. by W. Lee, H. Kanamori, P. Jennings, C. Kisslinger (Elsevier, Amsterdam, 2002)
3. F. Stacey, *Physics of the Earth* (Wiley, New York, 1969)
4. D. Anderson, in *Latest information from Seismic Observations*, ed. by T. Gaskell (Academic Press, New York, 1967)
5. M. Toksöz, M. Chinnery, D. Anderson, *Geophys. J. R. Astron. Soc.* **13**, 31 (1967)
6. B. Gutenberg, *Trans. Am. Geophys.* **39**, 486 (1958)
7. A.M. Dziewonski, D.L. Anderson, *Phys. Earth Planet. Inter.* **25**, 297 (1981)
8. L. Stixrude, C. Lithgow-Bertelloni, *Geophys. J. Int.* **162**, 610 (2005)
9. D.C. Rubie, T.S. Duffy, E. Ohtani, *Phys. Earth Planet. Inter.* **143–144**, 1 (2004)
10. J. Ganguly, A.M. Freed, S.K. Saxena, *Phys. Earth Planet. Inter.* **172**, 257 (2009)
11. D.H. Green, A.E. Ringwood, *J. Geophys. Res.* **68**, 937 (1963)
12. T. Katsura, E. Ito, *J. Geophys. Res.* **94**(B11), 15663 (1989)
13. A.L. Dergachov, V.I. Starostin, *Ore Depos. Geol.* **6**, 67 (1981)
14. S. Arafin, R.N. Singh, A.K. George, A. Al-Lazki, *J. Phys. Chem. Solids* **69**, 1766 (2008)
15. O. Anderson, *Equations of State of Solids for Geophysics and Ceramic Science* (Oxford University Press, New York, 1995)
16. C.M.R. Fowler, *The Solid Earth: An Introduction to Global Geophysics* (Cambridge University Press, New York, 1990)
17. A.K. George, R.N. Singh, S. Arafin, C. Carboni, S.H. Al-Harhi, *Physica B* **405**, 4586 (2010)
18. J.H. Perepezko, J.S. Paik, *J. Non Cryst. Solids* **113**, 61 (1984)
19. T. Shen, J.T. Wang, *J. Non Cryst. Solids* **559**, 117 (1990)
20. R.N. Singh, F. Sommer, *Phys. Chem. Liq.* **129**, 28 (1994)